XVI International Conference on Computational Plasticity. Fundamentals and Applications
COMPLAS 2021
E. Oñate, D. Peric, M. Chiumenti and Eduardo de Souza Neto (Eds)

EXPERIMENTAL AND NUMERICAL CHARACTERIZATION OF PLASTICITY AND FRACTURE BEHAVIOR OF ALUMINUM 6061-T4 SHEET FOR DEEP DRAWING SIMULATION

SHEIKH ENAMUL HOQUE*, FABIAN DUDDECK†

* LKR Light Metals Technologies Ranshofen
AIT Austrian Institute of Technology
Lamprechtshausener Str. 61, 5282 Ranshofen, Austria
Email: sheikh.hoque@ait.ac.at, https://www.ait.ac.at

† Department of Civil, Geo and Environmental Engineering
Technical University of Munich
80333 Munich, Germany
Email: duddeck@tum.de https://www.bgu.tum.de/cm/

Key words: MAT36, GISSMO, Xue-Wierzbicki, Sheet Metal Forming Simulation.

Abstract. A hybrid experimental-numerical approach is employed to characterize the plasticity and fracture properties of 1.0 mm thick aluminum 6061-T4 sheets. The experimental program consists of various tests corresponding to different stress states ranging from simple shear up to plane strain tension. The anisotropic elasto-plastic behavior is characterized by a modified Barlat89 model (MAT36E) in the commercial finite element solver LS-DYNA. The stress state dependent ductile fracture behavior is modeled with the Xue-Wierzbicki fracture criteria, which is implemented into the phenomenological damage model GISSMO in LS-DYNA. A deep drawing experiment is performed for the validation of the material card. The FE-simulation of the deep drawing experiment using the calibrated material card is able to predict the onset of fracture accurately.

1 INTRODUCTION

To reduce CO2 emissions in the automotive and aerospace sector, lightweight optimal design of structures is inevitable. One way of achieving lightweight design is to push the design limit of the material properties. For decades, the onset of necking, namely Forming Limit Curve (FLC), has been used as the design limit in deep drawing [1-8]. Today, engineers are often interested in the response of sheet metals in the post-necking range all the way up to fracture. Hence, accurate characterization of the ductile fracture behavior of sheet metal is crucial.

One approach for modeling ductile fracture is using conventional nonporous plasticity models in conjunction with a damage indicator. Such a damage indicator framework, widely used and commercially available, is GISSMO (Generalized Incremental Stress State dependent damage MOdel) [9]. In plane stress condition, e.g. for shell elements, GISSMO allows the input of the failure strains in the space of stress triaxiality in a tabulated form. Hence, any stress triaxiality (η) dependent fracture model [10-13] can be implemented in GISSMO.

The parameter identification of the fracture models involves a set of specimen tests covering

a wide range of stress triaxiality. In plane stress condition, the triaxiality ranges from -0.67 up to 0.67. It has been shown in [15] that fracture never occurs below a stress triaxiality of -0.33. Four distinct stress triaxialities within this range (-0.33 to 0.67) are: shear (η=0.0), uniaxial tension (η=0.33), plane strain tension (η=0.58) and equi-biaxial tension (η=0.67).

For accurate prediction of fracture behavior, an appropriate plasticity model capable of describing the elasto-plastic behaviour of the sheet metal is a prerequisite. Typically, sheet metals exhibit significant anisotropy due to their crystallographic structure and the characteristics of the rolling process. In order to capture this behavior, many plasticity models have been proposed over the past decades. A comprehensive description on different plasticity models can be found in [19].

In this work, a modified Barlat89 model [17, 18] is found to be reasonably accurate to describe the elasto-plastic behavior of the sheet metal under investigation. The Xue-Wierzbicki fracture model [14] is implemented in GISSMO. The parameter identification of the Xue-Wierzbicki fracture model is done based on a shear test ($\eta\approx0$), a flat tensile test with central hole ($\eta\approx0.33$) and a notched tensile test ($\eta\approx0.58$). Since the fracture parameters cannot be obtained directly from specimen tests, an experimental-numerical hybrid approach based on [16] is followed. After identifying the plasticity and fracture parameters, a deep drawing simulation is performed in LS-DYNA. Finally, the accuracy of the material card is validated by comparing the onset of fracture observed in the simulation with that in the deep drawing experiment.

2 EXPERIMENTAL WORK

Six different specimen geometries are cut (Figure 1) from 1.0 mm thick EN AW-6061 T4 aluminum sheet. The specimens are: Uniaxial Tension (UT-$L_0$80), Shear (SH), Central Hole (CH), and Notched Tension (NT) with three different notch radii, e.g. 20 mm (NT20), 10 mm (NT10), and 5 mm (NT5). The detailed information about the specimen geometries can be found in [16, 20, 21]. All the specimens are tested at room temperature under quasi-static loading condition with a strain rate of 0.001/s.

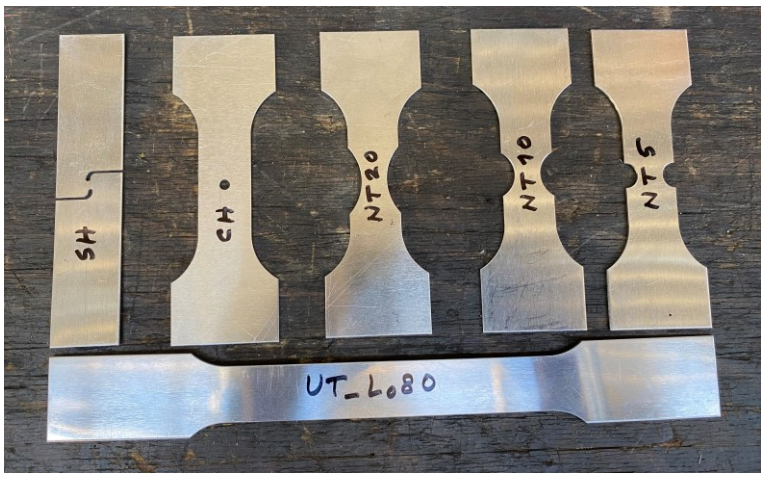

Figure 1: Specimen geometries

The UT specimens are cut in three different directions: 0° (UT00), 45° (UT45), and 90°

(UT90) with respect to the rolling direction. All other specimens are cut only in the rolling direction. Three specimens are tested for each sample geometry to ensure the repeatability of the tests.

3 MATERIAL PARAMETER IDENTIFICATION

3.1 Plasticity

The hardening curves and the Lankford coefficients in three different directions (0°, 45° and 90° to the rolling direction) of the sheet material are obtained through standard uniaxial tension experiments (UT-$L_0$80). A mild variation of the hardening curves (UT00, UT45, UT90) and the Lankford coefficients (r00, r45, r90) with the angle to the rolling direction is observed (Figure 2).

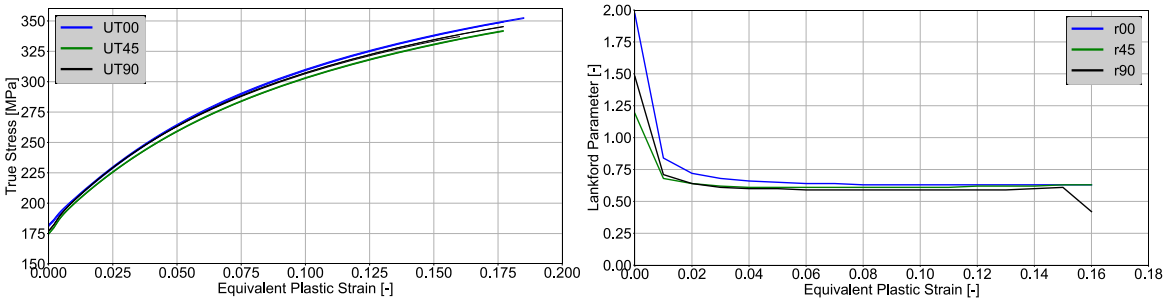

Figure 2: (left) Hardening curves and (right) Lankford coefficients in 0°, 45° and 90° to the rolling direction

The hardening curves obtained from uniaxial tension tests are only valid up to the point of diffuse necking. In our case, the plastic strain is approximately 0.18 (Figure 2). Since in deep drawing, the sheet metal goes through large plastic deformations, the stress-strain relationship only up to the diffuse necking is not enough for numerical simulation. Hence, the hardening curves in different directions for high plastic strain range is determined by an inverse iterative method [22].

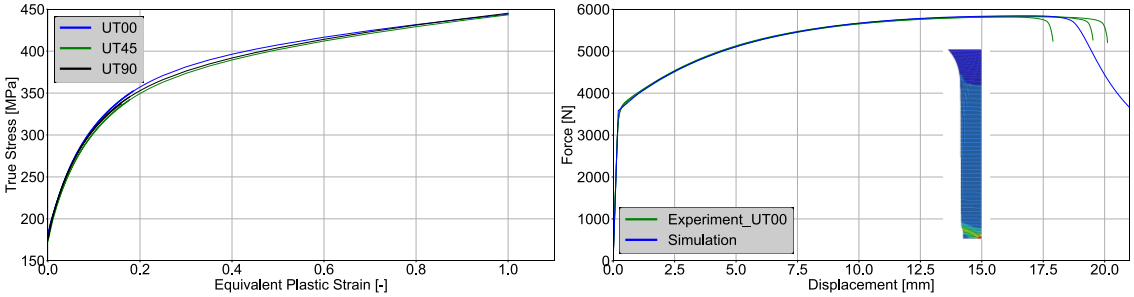

Figure 3: (left) Experimentally determined hardening (thick lines) and calibrated hardening (thin lines) determined by inverse iterative method, (right) comparison between experiment and simulation for UT00

At first, each hardening curve is fitted and subsequently extrapolated using Hockett-Sherby [23] and Swift [24] hardening law. Then, the uniaxial tension test is simulated using both extrapolations and their different combinations iteratively until the force-displacement curve of

the uniaxial tension test simulation fits well with that of the experiment. Local strain distributions from DIC (Digital Image Correlation) measurements may be used to further increase accuracy of the calibration, but such experiments are beyond the scope of our paper.

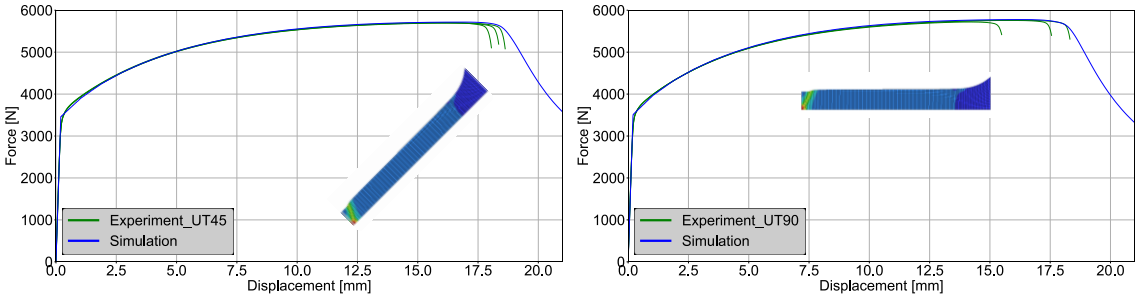

Figure 4: Comparison between experiment and simulation for UT45 (left) and UT90 (right)

The Lankford parameters (Figure 2, right) have very high initial values which is unrealistic. Hence, they are averaged between a plastic strain range of 0.02 and 0.15. The average values are: r00=0.65, r45=0.62, r90=0.60.

3.2 Fracture

Three specimens (SH, CH and NT5) are used in the determination of the fracture parameters of the Xue-Wierzbicki model. Each specimen is modeled in LS-DYNA using 0.5 mm fully integrated shell elements (elform16). Symmetric boundary conditions are used in order to reduce calculation time. Explicit time integration scheme in LS-DYNA is used for the simulations.

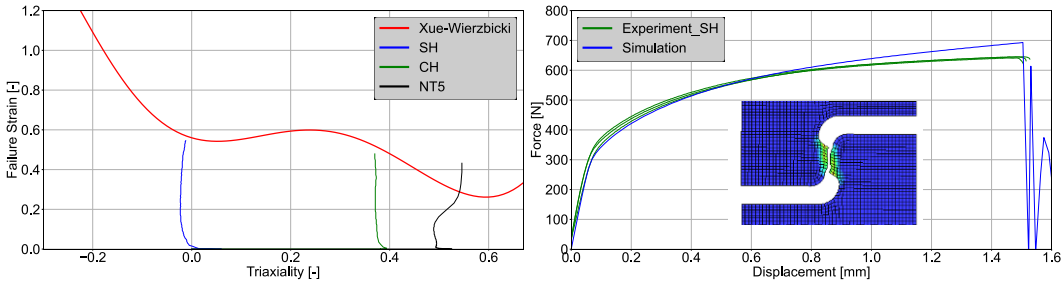

Figure 5: (left) Strain histories of critical elements and the final failure curve, (right) comparison between experiment and simulation of SH specimen

Initially, each specimen test is simulated without using any fracture model. From these simulations, the strain histories of the critical elements of each specimen are plotted (Figure 5, left). These histories give us an idea about the failure strains at corresponding stress states, depending on the nonlinearity of the strain history. Then, the Xue-Wierzbicki fracture model is fitted through the failure strains as a starter.

In the next step, all three simulations are carried out simultaneously and iteratively while the Xue-Wierzbicki model parameters are adjusted in each iteration until the experiments and the simulations agree reasonably well (Figure 5, right and Figure 6). The failure curve obtained by this iterative process is now valid for a mesh size of 0.5 mm. This element size is too small at

the component level, e.g. deep drawing simulation. Hence, a regularization is done in order to eliminate the mesh sensitivity.

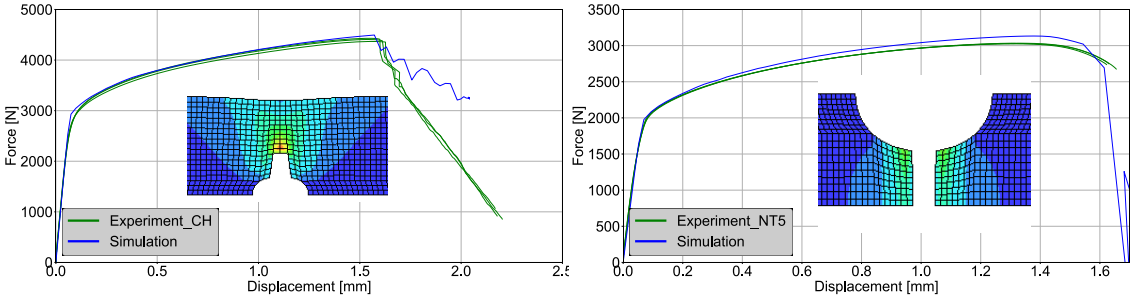

Figure 6: Comparison between experiment and simulation of CH specimen (left) and NT5 specimen (right)

The NT20 specimen is used in the mesh regularization, since none of the three specimens (SH, CH, NT5) used in the failure curve calibration can be meshed with large element size. The NT20 specimen is discretized with three different mesh sizes: 1 mm, 2 mm and 3.3 mm (Figure 7).

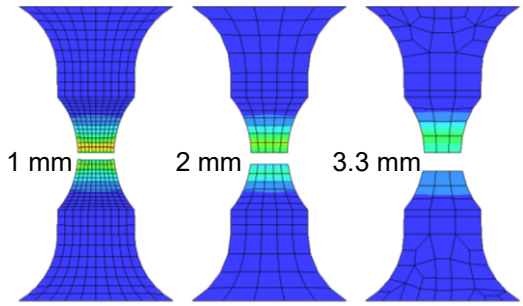

Figure 7: NT20 specimen meshed with three different element sizes for regularization

The regularization factor for each mesh size is determined by iterative simulations until all the simulations using different mesh sizes agree reasonably well with the experiment (Figure 8, right).

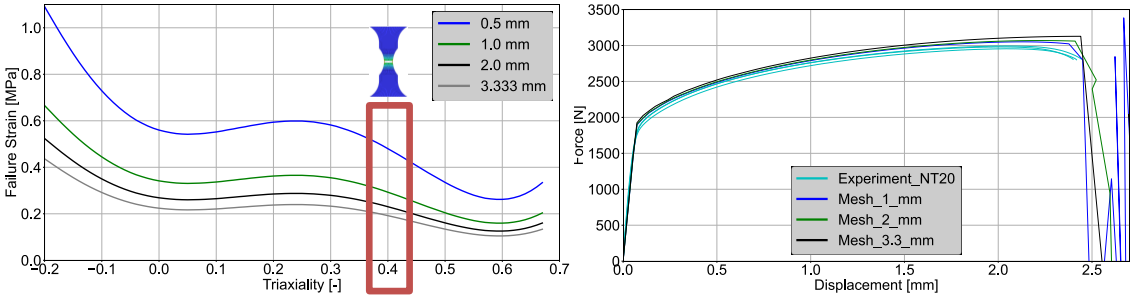

Figure 8: (left) Regularized failure curves, (right) experiment vs. simulation for NT20 specimen

The stress triaxiality of NT20 specimen varies approximately between 0.35 and 0.45, which ensures the accuracy of the above regularization procedure only for that triaxiality region. There

is no guarantee that the regularization is also accurate enough for triaxialities farthest away from this range, e.g. shear (triaxiality=0) and equi-biaxial tension (triaxiality=0.67). In fact, often it is assumed that there is no strain localization, and hence, no mesh sensitivity under shear stress state [9]. Additionally, after carrying out numerical simulations of the equi-biaxial test using different mesh sizes, only little mesh dependency has been observed [9]. This means the mesh regularization under shear and equi-biaxial tension stress state should be deactivated (Figure 9, right).

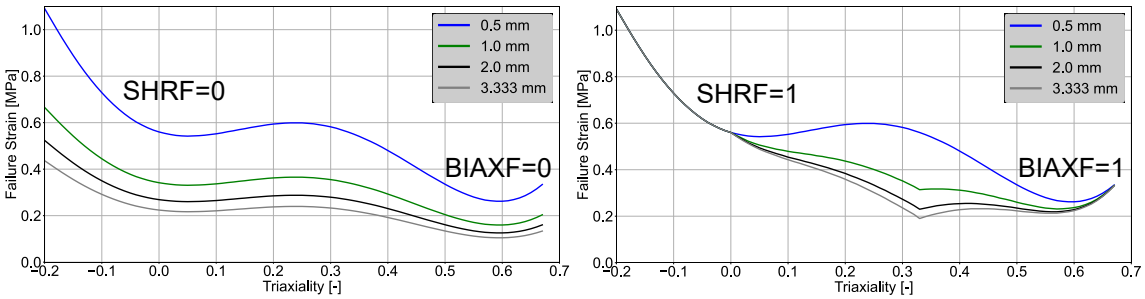

Figure 9: Regularization under shear and equi-biaxial stress state is activated (left) and deactivated (right)

4 DEEP DRAWING SIMULATION AND EXPERIMENTAL VALIDATION

A cross-die deep drawing simulation is performed using the material parameters identified in the previous section. The blank is meshed with 3 mm fully integrated shells (elform16). The tool was modeled as rigid body. Zero friction is assumed between the tool and the blank in the simulation, since lubricant is used in the experiment to reduce friction. The draw depth at onset of fracture in the simulation and in the experiment agree very well with each other, although the location does not match perfectly (Figure 10).

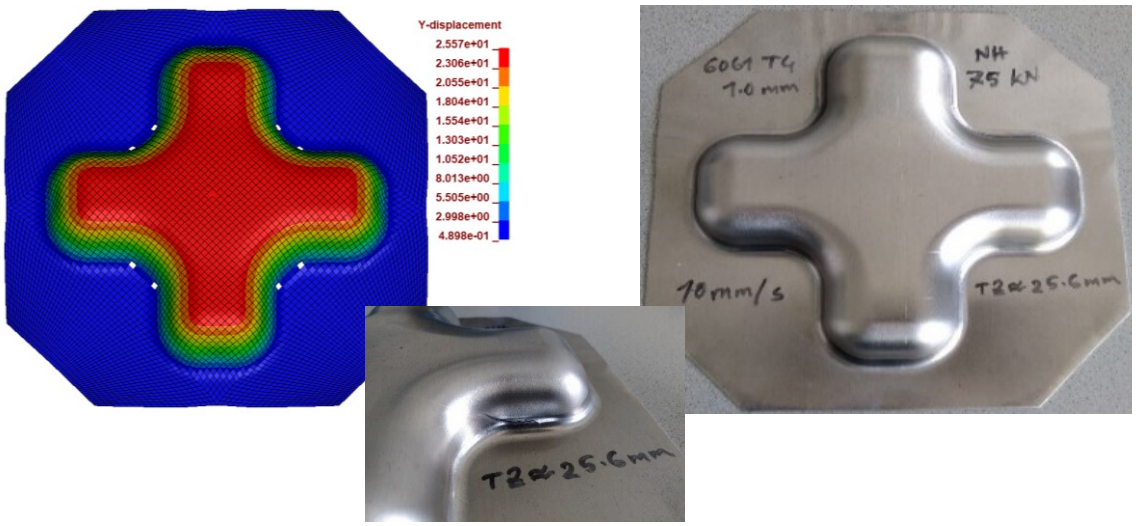

Figure 10: Deep drawing simulation vs experiment, both at onset of fracture

Another simulation is carried out while activating the regularization under shear and equi-biaxial stress state. A significant amount of fracturing is observed which does not correlate with

the experiment at all (Figure 11).

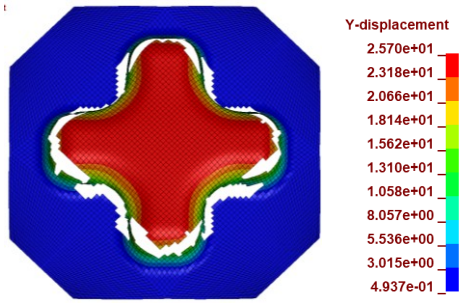

Figure 11: Deep drawing simulation with regularization under shear and equi-biaxial stress state activated

5 CONCLUSIONS

The anisotropic elasto-plastic behavior of aluminum 6061-T4 sheet is characterized by an extended Barlat89 model. The hardening curves are extrapolated using mixed Swift and Hockett-Sherby hardening laws and calibrated by an iterative inverse method. The ductile damage and fracture behaviors are modeled with GISSMO and the Xue-Wierzbicki fracture model respectively. Reasonably good agreement is observed between the deep drawing simulation and the experiment in terms of the onset of fracture. An equi-biaxial test could be included in the fracture calibration procedure for better certainty. Additionally, DIC measurements can be incorporated for better understanding of the strain localization.

12 ACKNOWLEDGEMENTS

This work has been partially supported by the European Regional Development Fund (EFRE) in the framework of the EU-program "IWB Investition in Wachstum und Beschäftigung Österreich 2014-2020", and the federal state Upper Austria.

The authors would also like to thank the State of Upper Austria for partial financial support of this research work in the frame of the project PSHeRo:ER (\#Wi-2020-700757/4-Höf) within the strategic program ‘upperVISION2030’.

REFERENCES

[1] Nakazima K, Kikuma T and Hasuka K. Study on the formability of steel sheets. YAWATA Tech Rep (1968); 264:8517–8530.

[2] Banabic D, Lazarescu L, Paraianu L, Ciobanu I, Nicodim I and Comsa DS. Development of a new procedure for the experimental determination of the forming limit curves. CIRP Ann Manuf Technol (2013); 62(1):255–8.

[3] Wang H, Yan Y, Han F and Wan M. Experimental and theoretical investigations of the forming limit of 5754O aluminum alloy sheet under different combined loading paths. Int J Mech Sci (2017); 133:147–66.

[4] Marciniak Z and Kuczyński K. Limit strains in the processes of stretch-forming sheet metal. Int J Mech Sci (1967); 9(9):609IN1613–122620.

[5] Hill RT. On discontinuous plastic states, with special reference to localized necking in thin sheets. J Mech Phys Solids (1952); 1(1):19–30.

[6] Swift H. Plastic instability under plane stress. J Mech Phys Solids (1952); 1(1):1–18.
[7] Hora P and Tong L. Prediction methods for ductile sheet metal failure using FE-simulation. In: Proceedings of the IDDRG congress (1994); p.363–75.
[8] Stoughton TB and Yoon JW. A new approach for failure criterion for sheet metals. Int J Plast (2011); 27(3):440–59.
[9] Andrade F X C, Feucht M, Haufe A and Neukamm F. An incremental stress state dependent damage model for ductile failure prediction. Int. J. of Fracture (2016); 200:127–150.
[10] Bao Y and Wierzbicki T. On fracture locus in the equivalent strain and stress triaxiality space. Int J Mech Sci (2004); 46(1):81–98.
[11] Bai Y and Wierzbicki T. Application of extended Mohr–Coulomb criterion to ductile fracture. Int J Fract (2010); 161(1):1–20.
[12] Lou Y and Huh H. Prediction of ductile fracture for advanced high strength steel with a new criterion: experiments and simulation. J Mater Process Technol (2013); 213(8):1284–302.
[13] Mohr D and Marcadet SJ. Micromechanically-motivated phenomenological Hosford—Coulomb model for predicting ductile fracture initiation at low stress triaxialities. Int J Solids Struct (2015); 67:40–55.
[14] Wierzbicki T, Bao Y, Lee Y-W and Bai Y. Calibration and evaluation of seven fracture models. International Journal of Mechanical Sciences (2005); 47:719–743.
[15] Bao Y and Wierzbicki T. On the cut-off value of negative triaxiality for fracture. Engineering Fracture Mechanics (2005); 72:1049–1069.
[16] Dunand M and Mohr D. Hybrid experimental–numerical analysis of basic ductile fracture experiments for sheet metals. International Journal of Solids and Structures (2010); 47:1130–1143.
[17] Barlat F and Lian K. Plastic behavior and stretchability of sheet metals. Part I: A yield function for orthotropic sheets under plane stress conditions. International Journal of Plasticity (1989); 5(1): 51-66.
[18] N.N. LS-DYNA Keyword User's Manuel, Volume II: Material Models (09/08/2020).
[19] Banabic D. Sheet Metal Forming Processes: Constitutive Modelling and Numerical Simulation, Springer-Verlag Berlin Heidelberg (2010).
[20] DIN 50125: Testing of metallic materials – Tensile test pieces (2016).
[21] Peirs J, Verleysen P and Degrieck J. Novel Technique for Static and Dynamic Shear Testing of Ti6Al4V Sheet. Experimental Mechanics (2012); 52:729–741.
[22] Zhao K, Wang L, Chang Y, Yan J. Identification of post-necking stress-strain curve for sheet metals by inverse method. Mechanics of Materials (2016); 92:107–118.
[23] Hockett J E, Sherby O D. Large strain deformation of polycrystalline metals at low homologous temperatures. In: Journal of the Mechanics and Physics of Solids (1975); 23:87–98.
[24] Swift HW. Plastic instability under plain stress. In: Journal of Mechanics and Physics of Solids (1952); 1:1–18.